Astrobiology
August 2019, Volume 19 Issue 8 Pages 1063-1074
https://doi.org/10.1089/ast.2018.1896
https://archimer.ifremer.fr/doc/00601/71306/

Photochemistry on the Space Station-Aptamer Resistance to Space Conditions: Particles Exposure from Irradiation Facilities and Real Exposure Outside the International Space Station

Coussot Gaelle [1, *], Le Postollec Aurelie [2], Incerti Sebastien [3], Baque Mickael [4], Faye Clement [5], Vandenabeele Trambouze Odile [6], Cottin Herve [7, 8], Ravelet Corinne [9], Peyrin Eric [9], Fiore Emmanuelle [9], Vigier Flavie, Caron Jerome [10], Chaput Didier [11], Przybyla Bartos [12], Berger Thomas [12], Dobrijevic Michel [2]

[1] Univ Montpellier, ENSCM, CNRS, IBMM, F-34093 Montpellier 5, France.
[2] Univ Bordeaux, B18N, CNRS, LAB, Pessac, France.
[3] Univ Bordeaux, UMR 5797, CENBG, Gradignan, France.
[4] German Aerosp Ctr DLR, Inst Planetary Res Management & Infrastruct, Res Grp Astrobiol Labs, Berlin, Germany.
[5] Colcom, Cap Alpha, Clapiers, France.
[6] UBO, LMEE, IUEM UMR 6197, Plouzane, France.
[7] Univ Paris Est Creteil, UMR 7583, LISA, Creteil, France.
[8] Univ Paris Diderot, Inst Pierre Simon Lapl, Creteil, France.
[9] Univ Grenoble Alpes, Dept Pharmacochim Mol, CNRS, UMR 5063, St Martin Dheres, France.
[10] Comprehens Canc Ctr, Inst Bergonie, Dept Radiotherapie, Bordeaux, France.
[11] Ctr Natl Etud Spatiales, DCT ME EM, Toulouse, France.
[12] German Aerosp Ctr, Inst Aerosp Med, Cologne, Germany.

* Corresponding author : Gaelle Coussot, email address : gaelle.coussot@umontpellier.fr

Abstract :

Some microarray-based instruments that use bioaffinity receptors such as antibodies or aptamers are under development to detect signatures of past or present life on planetary bodies. Studying the resistance of such instruments against space constraints and cosmic rays in particular is a prerequisite. We used several ground-based facilities to study the resistance of aptamers to various types of particles (protons, electrons, neutrons, and carbon ions) at different energies and fluences. We also tested the resistance of aptamers during the EXPOSE-R2 mission outside the International Space Station (ISS). The accumulated dose measured after the 588 days of this mission (220 mGy) corresponds to the accumulated dose that can be expected during a mission to Mars. We found that the recognition ability of fluorescently labeled aptamers was not significantly affected during short-term exposure experiments taking into account only one type of radiation at a time. However, we demonstrated that the same fluorescent dye was significantly affected by temperature variations (-21 degrees C to +58 degrees C) and storage throughout the entirety of the ISS experiment (60% of signal loss). This induced a large

variability of aptamer signal in our analysis. However, we found that >50% of aptamers were still functional after the whole EXPOSE-R2 mission. We conclude that aptamer-based instruments are well suited for in situ analysis on planetary bodies, but the detection step requires additional investigations.

Keywords : Astrobiology, Cosmic rays, Biochip, Aptamers

I. Introduction

In the context of planetary exploration, space agencies call for the development of miniaturized techniques to search for traces of extant or extinct life. In particular, the use of instruments based on bio-affinity receptors, like antibodies or aptamers, might be very efficient. In this technology, bio-affinity receptors are fixed to a solid surface to specifically capture their target. A signal is displayed when receptor-target recognition events occur.

Antibody-based biochips have been extensively studied in proteomic and functional genomics and their scope has been extended to the field of astrobiology. Indeed, due to the benefits of high throughput and miniaturization, and small volume consumption, antibody-based biochips have been proposed to detect biomarkers, especially organic ones, in the search for extraterrestrial life (Parro *et al.,* 2005; Le Postollec *et al.,* 2007; Parro *et al.,* 2008; Martins *et al.*, 2011; Parro *et al.*, 2011b; Sims *et al*., 2012; McKay *et al.,* 2013; Smith *et al.,* 2014). Space is a hazardous environment, with high fluxes of ionizing radiations, from primary particles of galactic cosmic radiation (GCR) and solar energetic particles (SEP), to secondary particles produced by the interaction of primary particles with environment materials. One main concern relies on the resistance of biochips to the cumulative effects of these radiations. In recent years, studies have been performed to evaluate the resistance of antibody reagents to space constraints, especially regarding the effect of specific particles on antibody binding performances (Le Postollec *et al.,* 2009a; Le Postollec *et al.,* 2009b; Baqué *et al.,* 2011a; de Diego-Castilla *et al.,* 2011; Baqué *et al*., 2017; Coussot *et al.,* 2017). To complement ground-based radiation studies, a short term mission was performed on the BIOPAN-6 low-earth orbit platform to demonstrate the effects of cumulative radiations on the antibodies' ability to bind to their respective antigens (Derveni *et al.*, 2012; Derveni *et al.,* 2013). For the absorbed radiation doses during the 12 days of exposure, the freeze-dried antibodies packaged into laser-cut glass fiber pads were unaffected

with regard to their recognition performances in the condition of the experiment. Furthermore, in the frame of the BiOMAS project (Biochip for Organic Matter Analysis in Space) and part of the Photochemistry on the Space Station (PSS) experiment, biochip models, in which antibodies were immobilized onto a surface, have been installed outside the International Space Station (ISS) on the EXPOSE-R2 platform, for a real long-term exposure (more than 18 months) to spatial constraints (Vigier *et al.,* 2013; Cottin *et al.* 2015, Cottin *et al.* 2017). Our recent results show that our biochip models resist to an 18 months extra-vehicular mission (Coussot *et al.,* 2018b). This work, in combination with the ground-based radiation studies, permits to assess the antibodies' ability to bind to their respective antigens even after a long-term exposure to the real space environment. These experiments indicated that antibody-based instruments seem well suited for the search for organic matter in *in situ* planetary bodiesô samples.

Other target-binding reagents with specificity and binding affinity rivalling with those of antibodies are aptamers. Aptamers are short, single-stranded nucleic acids, able to bind from small molecular weight molecules up to proteins. Aptamers have demonstrated some interesting advantages over antibodies: production at low cost, specificity against small and non-immunogenic molecules, thermal stability, and ability to maintain their structures over repeated cycles of denaturation/renaturation (Song *et al.* 2012). From diagnostics to food safety or therapeutics, aptamers have shown their interests in arrays and biosensors development (Song *et al.* 2012; Dong *et al.,* 2014; Rozenblum *et al.,* 2016; Gotrik *et al.,* 2016). The first investigation for nucleic acid aptamers ability to maintain their binding performances under simulated cosmic radiations, in particular 2 MeV protons effects, was carried out by Baqué *et al.* (2011b). The results revealed that, under the protons flux and energy tested, there were no deleterious effects on the binding affinity of the irradiated DNA aptamer. So far, no more

104 investigations on the effect of high-energy particles on aptamer performances have been
105 reported.

106 In the present study, we first present a set of experiments carried out these last seven years in
107 ground-based particles accelerator facilities to study the effect of different types of incident
108 particles (protons, electrons, neutrons, and carbon ions) at different energies and fluences, on
109 the ability of a model aptamer to recognize its target. The second part of the paper discusses the
110 results obtained after a long time exposure to real space constraints of aptamer samples in the
111 framework of the PSS project (Cottin *et al.*, 2015).

112

113

II. Materials and methods

II.1 Chemical, reagents and materials

L-tyrosinamide (*L*-Tym), fluorescein dye (F), sodium bicarbonate ($NaHCO_3$, Ó99,5%), sodium carbonate (Na_2CO_3, Ó 99,5%), and Tris(hydroxymethyl) aminomethane (TrisÓ 99,8%) were purchased from Sigma Aldrich (Saint-Quentin Fallavier, France). NaCl and $MgCl_2$ of analytical grade were obtained from Chimie-Plus Laboratoires (Bruyères de Pouilly, France) and Panreac Quimica (Barcelona, Spain), respectively. The aptamer anti-*L*-Tym containing 49 nucleotides and modified in its 3ô end by fluorescein (#4551724, MW 15 860.5 g/mol) was provided by Eurogentec (Angers, France). This aptamer was chosen as an aptamer model, it has been reported as 49merYm3ôF in the text, and had the following sequence 5ô-AATTCGCTAGCTGGAGCTTGGATTGATGTGGTGTGTGAGTGCGGTGCCC-F-3ô (4 different batches were used: batch 1 for ground-based neutrons, electrons, and protons experiments, batch 2 for ground-based ^{12}C experiments, batch 3 for ISS mission; batch 4 for post-flight experiments). The ultrapure water (18.2 MΩ) was obtained from a Purite Still Plus water purification system (Thame, UK). Other chemicals are analytical grade and used as received. Nunc MaxiSorpÊ polystyrene 96 well plates were obtained from VWR (France), and were used as sample containers during the freeze-drying step, and throughout the laboratory radiation exposures. In case of ISS experiment, Corning DNA BindÊ 8-well strip plate with N-hydroxysuccinimide modified surface (NHS-wells) were provided by Sigma Aldrich (Saint-Quentin Fallavier, France). NHS-wells were manufactured by Air Liquide (Sassenage, France) to fit perfectly with the shape and size of EXPOSE-R2 closed cells provided by the French Space Agency (CNES, Toulouse) (Vigier *et al.*, 2013). The home-designed NHS-wells had a diameter of 8.4 mm with a 7.1 mm height. Teflon cap were specially manufactured by Air Liquide to close the well. **(Figure 1a)**

138

139 ***II.2 Freeze-drying and sample preparation***

140 Particle irradiation effects were evaluated on both freeze-dried 49merYm3ôF aptamer and
141 fluorescein dye. One hundred microliters of 49merYm3ôF aptamer or fluorescein solution at
142 500 nM in ultrapure water (dilution by 1/40 from a stock solution freshly prepared at 20 µM
143 from aptamer commercial vial) were put into MaxiSorpÊ wells (commercial or home-designed
144 well format) and freeze-dried according to a protocol optimized for the freeze-drying of small
145 volume of reactants (Coussot *et al.*, 2018a). Briefly, MaxiSorpÊ wells were put into a home-
146 made aluminium holder, and liquid nitrogen was added to freeze the samples. The aluminium
147 holder was then placed into the central part of a freeze-dryer with a top-press device (Christ
148 Alpha 2ï 4 from Martin Christ GmbH, Germany). Freeze-drying was performed overnight
149 (condenser temperature ī 85°C, vacuum 0.05 mbar). The chamber of the freeze-dryer was filled
150 with nitrogen gas before closing the sample-containing aluminium holder, which kept sealed
151 hermetically the samples and sheltered them from the moisture and light until its opening. The
152 opening of the aluminium holder was done in a glove box under a controlled atmosphere of
153 helium (10% He) in argon (Ar) provided by Air Liquide (Sassenage, France) to maintain a
154 relative humidity (RH) level of 10 to 15%. During our experiments, the RH and air temperature
155 were controlled using a thermohygrometer Testo 605-H1 (Testo, France). RH was 12±3% and
156 air temperature was 22.8±2.3°C. After opening the aluminium holder, freeze-dried samples
157 were sealed within a plastic bag using a vacuum sealing device FoodSaverÊ (Fischer
158 Scientific, France) and stored at 4°C in the dark until running laboratory irradiation
159 experiments.

160 In case of ISS experiments, 150 µL of carbonate buffer (pH 9.4, 0.1M) were added into the
161 home-designed NHS-wells to deactivate reactive sites. The incubation took place overnight at

room temperature. After successive water washings, 100 µL of 49merYm3ôF aptamer/fluoroscein solution at 500 nM, freshly prepared in ultrapure water, were pipetted into each well. The freeze-drying procedure was run as described above. After opening the aluminium holder in the above controlled atmosphere, freeze-dried samples were capped and directly transferred into the CNES closed cells using a tool vacuum suction pen (FFQ939 from Mayf's Online Shop, China). The CNES closed cells were then screwed with a final tightening of 0.7Nm using a torque screwdriver TorqueVario®-S (Wiha, Germany) **(Figure 1b)** (Vigier *et al.*, 2013). Soldering of the CNES cells and their integration to the sample carriers were done according to CNES internal procedures.

II.3 Experiments on ground-based particles accelerator facilities

The composition of cosmic rays is dominated by protons, electrons, alpha particles, and a small fraction of heavy ions (like carbon, oxygen and up to iron ions). Interactions of these primary particles with matter produce secondary particles like electrons and neutrons. So, experiments on ground-based facilities (producing protons, electrons, neutrons and carbon ions) have been performed to study the impact of GCR and SEPs on the affinity of the 49merYm3ôF aptamer towards its *L*-Tym target. The set of experimental conditions is summarized in **Table 1,** and detailed in Baqué *et al.*, 2017. These are considered as short-term exposure experiments taking into account only one type of radiation at a time to study the potential effects on the 49merYm3ôF aptamer-*L*-Tym bindings. All experiments were repeated at least 3 times per irradiation conditions in order to have 3 titration curves per analytical conditions. 6 replicates were prepared for fluorescein dye. Freeze-dried samples were irradiated directly in their sealed bags. The influence of the bag during irradiation experiments was simulated with GEANT4 Monte Carlo toolkit and demonstrated to be negligible (Baqué *et al.*, 2017). Controls are the reference samples that have been freshly prepared the day of analysis: they did not undergo

freeze-drying process, neither transportation nor storage at 4°C. We previously verified that freeze-drying does not induced any effects on binding curves nor in K_d value. So, controls (freshly prepared references) can be used in place of lyophilized-non-irradiated samples for ground-based experiment interpretations. Analyses were done by using fluorescence polarization (FP) assay for aptamers as described in section *II.7*, and in direct fluorescence for fluorescein dyes as described in section *II.6*.

II.4 Experiment outside the International Space Station (ISS)

Simulating radiation environment in Earth facilities is highly complicated, since it is almost impossible to include all constraints encountered during an entire space mission all together (long duration storage, transportation, take-off/landing shocks, thermal constraints, and cumulative effects of cosmic rays particles). For that purpose, 11 samples (7 ground controls, 4 exposed samples also denoted as ISS samples) took part in the ñBiochip in PSS experimentò (Vigier *et al.,* 2013; Cottin *et al.,* 2015) during the EXPOSE-R2 mission. These samples were simultaneously prepared, within the same freeze-drying batch, as that described in the paragraph *II.2*. The 4 exposed CNES cells were spread on the 2 exposure levels of the Tray 3 of the EXPOSE carrier dedicated to the PSS experiment. Disposition of the 2 CNES cells on the sample carrier were the same for the upper and the lower level of the sample carrier. Launch to ISS (July 23th, 2014) and storage inside ISS was at ambient temperature (22-25°C on average) (Rabbow *et al.,* 2017). Then, EXPOSE-R2 platform was placed outside the ISS on the Universal platform D on August 18th with opening of the valves on August 20th, and removal of the UV shield in October 22nd, 2014. On February 3rd 2016 trays were covered and brought back inside the ISS. Thus, the exposed samples spent 566 days outside the ISS over the 588 days of the mission (1 year, 8 months).

Into each CNES cell, two thermoluminescent detectors (TLDs) were placed at the bottom of the cell, below the samples. These passive dosimeters were analyzed at the end of the mission (for detailed methods of analysis see Berger *et al.*;2012; 2015) and revealed that the absorbed dose by our aptamer samples was about 220 mGy for the 588 days of the mission. This absorbed dose is consistent with doses expected for a mission to Mars. Indeed, considering Geant4 simulations in Le Postollec *et al*. (2009a), this absorbed dose (220mGy) corresponds to 8 months travel and 6 months at Mars surface. Considering doses measured by Curiosity rover (Hassler *et al*., 2014), this dose corresponds to a mission to Mars with 8 months travel and 18 months at the surface.

During their extravehicular exposition, the samples on Tray 3 were submitted to temperatures varying between -20.9°C and 57.98°C (Rabbow *et al.*, 2017). Accurate measurements of the CNES exposed cells temperature were provided by the temperature control interface of the Planetary and Space Simulation Facilities (Microgravity User Support Center (MUSC), http://www.musc.dlr.de/expose-r-2/; **Figure 2a**). On March 2nd 2016, EXPOSE-R2 Tray 3 landed on Earth. During transit from Baïkonur cosmodrome to Moscow, and from Moscow to German Aerospace Center (DLR, Germany) a recording of temperatures was done, the temperatures oscillated between 20°C and 24°C. Then from DLR to LISA (Laboratoire Interuniversitaire des Systèmes Atmosphériques, Paris Est-Créteil) (Rabbow *et al.*, 2017), and Paris to Montpellier a controlled chamber at 4°C was used during transportation in the summer period. De-integration of the exposed CNES cells from the sample carriers was done according to MUSC/DLR/ESA/CNES internal procedures. On June 24th 2016, the soldered joint of all the CNES cells (including ground references) was removed, using a mechanical lathe and a manufactured CNES tool, in the mechanics department of the Montpellier University (**Figure**

232 **1c**). Samples were immediately sealed in a FoodSaverÊ bag (Fischer Scientific, France) and
233 stored in the dark at 4°C until analysis with FP assays.

234 ***II.5 EXPOSE-R2 mission ground references***

235 During the same period, experiments have been performed on ground to control the long-term
236 behaviour of the 49merYm3ôF aptamer upon storage but not exposed to space constraints. Two
237 ground CNES cells were stored at the French Space Agency (CNES, Toulouse) by maintaining
238 an accurate temperature control at 3.9±0.8°C over that period. These samples were named as
239 ñCNES 5°Cò samples. Three ground CNES cells were kept in DLR (Cologne, Germany): 2
240 ground CNES cells were stored at 5°C (ñDLR 5°Cò samples) and 1 ground CNES cell
241 underwent the same thermal history as ISS samples (ñDLR æTò sample) (see above, **Figure**
242 **2a**). In addition, the behaviour of 2 additional ground samples was studied at DLR combining
243 long time storage, varying thermal environment as ISS ones, and UV radiations (ñDLR
244 æT+UVò samples) (Rabbow *et al.*, 2017). Calibrated Bentham 150 double monochomators
245 instrument equipped with a SOL2000 lamp (Dr. K.Hönle GmbH, Martinsried, Germany) was
246 used to provide a spectrum similar to that of sunlight. All of these 7 ground CNES cells were
247 brought back to Montpellier to be handled simultaneously with the exposed CNES cells during
248 all the desoldering process and 4°C storage (section *II.4*) before running FP assays (section
249 *II.7*). However, data of DLR æT and DLR æT+UV samples have not been added to our analysis
250 due to the lack of precision of the applied temperatures.

251 ***II.6 Additional ground thermal cycling experiments***

252 The 49merYm3ôF aptamer and fluorescein dye were freeze-dried at 500 nM in ultrapure water
253 as described in section *II.2*. Thermal cycling experiments were carried out on freeze-dried
254 samples in their sealed bags in a temperature test chamber (Vötsch VT 4004). Two independent

thermal variation experiments were done: one with a sharp rise in temperature (5°C/min) until a one hour plateau at 80°C (referred as ñ80°C peakò in the text), and a long cycling period (178.8 hours or 7.45 days) mimicking thermal variations of exposed cells (**Figure 2b**) with an amplitude of about 70°C (referred as ñlong cycleò in the text). After reconstitution of freeze-dried product with 120 µL of deionized water, 100 µL were pipetted into black 96-well half-area microplates from Greiner Bio-One (Courtaboeuf, France) to measure fluorescence intensity of the signal (RFS). Fluorescence measurements were done on a Tecanôs Infinite® F500 microplate reader (Mannedorf, Switzerland) having excitation and emission filters at 488 nm and 525 nm, respectively. A blank signal with neither aptamer nor fluorescein dye was used to evaluate noise value (RFN). Results are presented as signal to noise (S/N) ratio equals to RFS/ RFN.

II.7 Aptamer-based fluorescence polarization (FP) assay

For all experiments carried out in ground-based particles accelerator facilities and the overall ISS mission, a structure-switching aptamer assay based on a fluorescence polarization (FP) approach (**Figure 3**) was used to evaluate the binding ability of the 49merYm3ôF aptamer towards its *L*-Tym target. The approach, described by Ruta *et al.* (2009) and Perrier *et al.* (2010), is based on monitoring the fluorescence anisotropy change (ρ*r*) of an aptamer labelled by a single fluorescent dye at its 3ôend. Fluorescence anisotropy change ρ*r* was calculated as the difference between the measured anisotropy (*r*) of the labelled aptamer-target complex, and the anisotropy in absence of target (r_f), which was prepared by replacing the *L*-Tym target solution by deionized water. The optimized binding buffer for FP assay consisted of 10 mM Trisï HCl, pH 7.5, 10 mM $MgCl_2$ and 50 mM NaCl (Zhu *et al.*, 2011). The aptamer solutions (500 nM) were heated at 80°C for 5min for denaturation then left to stand at room temperature in the dark for 30min. 100 µL of the renatured aptamer solutions were deposited into black 96-

well half-area microplates containing the increasing concentrations of *L*-Tym (0.5/1/2.5/5/7.5/10or12.5/25.0/40.0or50.0/80.0/200.0µM) for measurements on Tecan's Infinite® M1000 PRO (Tecan, France). Excitation was set at 485±20 nm, and emission was collected with 535±25nm bandpass filters.

II.8. Data interpretation and statistical analysis

For a 1:1 stoichiometry, the measured anisotropy (r) can be linked to the apparent dissociation constant K_d via the following relation:

$$r = \frac{r_f K_d + r_b c}{K_d + c} \qquad \text{Eq (1)}$$

where r_f is the anisotropy in the absence of target, r_b the anisotropy of maximally target-associated aptamer, and c the concentration of free target. For a limiting aptamer probe concentration, the total concentration of target (c_T) in the reaction system approximates the free target concentration c. The nonlinear regression of the r versus c (å c_T) plots, where r_b and K_d constituted the adjustable parameters, was achieved using the Table curve 2D software (Systat Software Gmbh, Erkrath, Germany).

To evaluate cosmic rays effects on freeze-dried exposed aptamers, control samples were prepared with an aptamer probe that did not undergo freeze-drying process or irradiation (reference sample). Binding affinity data for exposed samples and control samples were compared using the relative dissociation constant value (relative K_d) expressed as follow:

$$\frac{K_{d\,(irradiated)}}{K_{d\,(control)}} \qquad \text{Eq (2)}$$

Relative K_d values are reported in **Table 2.**

For the ISS experiments, relative K_d were estimated from freeze-dried ground samples stored at 5°C in DLR facility during all the duration of the mission. ñFlight samplesò corresponded

301 to ISS samples that undergo all cumulative effects of the mission (flights, extravehicular
302 exposure, and transportation). Relative K_d values are reported in **Table 3.**
303 All data are reported as the mean ± the standard deviation (SD) from at least four replicate
304 experiments. Statistical significance of the assays was determined using Studentôs *t*-test
305 (p=0.05).
306

III. Results

We first determined a reference value of the affinity of the aptamer used to its target. In the various FP assays we performed, the concentration of 49merYm3ôF aptamer was constant (500 nM) and its target *L*-Tym increased in concentrations from 0.5 to 200 µM (10 levels of concentrations, see experimental part). Binding data of 49merYm3ôF aptamer to *L*-Tym were globally fit to four parameter logistic regressions permitting the calculation of K_d (1.54±0.14 µM, aptamer batches 1, 2, 3, n=14), which is comparable with previous published data (Ruta *et al.*, 2009).

III.1. Irradiation effects on aptamers during ground-based experiments

To minimize experimental error, all assays were performed at least in triplicate. Affinity curves do not reveal significant differences in anisotropy change œr **(Figure 4)**. The corresponding relative K_d values were calculated (*Eq. 2*), and reported in **Table 2**. The aim of the present study, according to the particle types, fluences, energies and exposure durations, is to determine whether irradiated samples undergo damaging effects on the aptamer leading to a decrease in its ability to bind to its target or leading to a decrease of the detection signal. Although no effect was detected with ^{12}C ions at high energy **(Figure 4a),** (statistically identical K_d values), differences in **œr** were observed with other particles. For instance, in **Figure 4b**, a slight difference was observed in ær between the two irradiated samples with electrons. However, analysis of the relative K_d for both irradiated samples shows that there were statistically identical (p>0.05) compared to the corresponding reference. This suggests that the recognition capabilities of the 49merYm3ôF aptamer were not affected by the irradiation process even when using higher fluence and irradiation duration. The same phenomenon was observed with neutrons: the higher fluence F_{n1} induced

a larger decrease in anisotropy change qpr **(Figure 4c).** The relative K_d value corresponding to irradiated sample with (F_{n1}; E_n; D_{n1}) radiation conditions (which presents higher variability), stayed statistically identical to the reference one. Consequently, we hypothesized that high fluences of electrons and neutrons might have deleterious effects on the fluorescein dye. To verify that point, we run a Student's *t*-test on fluorescence intensities obtained for fluorescein dye before and after irradiations. It revealed that significant differences could be observed with up to 40% loss in fluorescence signal for high fluence F_{n1} for neutrons and fluence F_{p1} at both energies E_{p1} and E_{p2} for protons. So, potential degradation of fluorescein dye might occur with higher fluence. Thus, after exposure to (F_{e1}; E_e; D_{e1}) radiation with electrons beam and (F_{p1}; E_{p1}) et (F_{p1}; E_{p2}) radiation with protons beam, fluorescence anisotropy changes might not be due to alteration of binding but rather suggest some alterations of the fluorescein dye emitting properties. In addition, with protons, cumulative effects were observed. Indeed, the results of FP measurements after protons irradiation showed a small discrepancy between the reference sample and the 4 irradiated ones **(Figure 4d).** Although K_d values were slightly smaller than that of the reference **(Table 2)**, they remained statistically identical. All radiation configurations tested led to a similar anisotropy change qpr that could suggest there was no important damage in the structure of the 49merYm3ôF aptamer that consequently could alter the binding to its target *L*-Tym. Compared to our previous published data (Baqué *et al*., 2011b), showing that 2MeV protons had no effect on the binding affinity of irradiated 49merYm3ôF aptamer neither on the fluorescein dye, the present data might suggest that higher energies of protons (25 MeV/50 MeV) alter the fluorophore.

III.2. ISS experiments

Since radiation gradients were observed on the EXPOSE platform in previous ISS missions (Berger *et al*., 2012; 2015), the 4 exposed aptamers ñFlight samplesò were spread on the 2 exposure levels of the Tray 3 of the EXPOSE carrier dedicated to the PSS experiment, but with the same disposition on the upper and lower level of the sample carrier. However, measurements performed with passive dosimeters during the EXPOSE-R2 mission revealed, a posteriori, that the absorbed dose difference between cells at upper and lower levels was extremely low (about 3 mGy for the whole mission corresponding to 1.4% of the total). Some TLDs stacks composed of eleven TLDs included into Tray 3 structure bring explanations on this very low difference. As can be seen in **Figure 5**, absorbed dose decreases when shielding increases but after ~ 0.75 g/cm^2 of shielding, the absorbed dose measured remains quasi stable and the dose decrease evolves very slowly even if shielding is significantly increased. As the estimated shielding of TLDs placed into cells on the upper level is about 0.82 g/cm^2, it explains the very low absorbed dose difference observed between both levels.

Calculation of K_d from independently and freshly prepared reference samples was 1.58±0.12 µM (aptamer batch 4), which is comparable with the above reference value (1.54±0.14). However, K_d values from the 8 mission samples appeared to be on average 1.5-2 times higher. We previously verified that freeze-drying induced no effects on binding curves nor in K_d value. However, storage stability analyses of freeze-dried 49merYm3ôF aptamer (batches 1&2), carried out at 4°C for 20 days and 7 months, showed differences in anisotropy change ¢r for the different storage times and aptamer batches (data not shown). Consequently, to only take into account the effects encountered during the ISS mission (flights, extravehicular exposure, and all transportations during the mission) relative K_d were calculated using the freeze-dried ground samples stored at 5°C in DLR facility during all the duration of the mission. The binding

curves and the corresponding relative K_d values are reported in **Figure 6** and **Table 3**, respectively. We distinguished two groups of affinity curves. Group1 concerns the highest measured anisotropy change qpr with both ground controls stored at 5°C (DLR and CNES) during the mission. Group 2 represents the flight samples. We note that the ñlower trayò samples seem to have a different behaviour than the flight samples exposed in the ñupper trayò.

Based on these observations, an effect due to the temperature variations during the mission can be invoked. To test this hypothesis, post-flight ground thermal cycling experiments were carried out on the 49merYm3ôF aptamer and the fluorescein dye over a 80°C short peak of temperature and a long cycle mimicking thermal variations of flight samples (see *section II.6* of the experimental part and **Figure 2b**). S/Ref values were 74.5±15.1, 62.1±23.5, and 59.0±14.9 for the freeze-dried fluorescein reference, the 80°C peak, and long cycle, respectively. The aptamer S/Ref values were 23.3±5.9, 23.5±10.4, and 70.6±20.8 for the reference, the 80°C peak, and long cycle, respectively. Consequently, there is no great impact of thermal variation upon the fluorescence properties of the freeze-dried dye. On the contrary, significant differences were observed with the 49merYm3ôF aptamer, with the same order of S/Ref for the long cycle (70.6±20.8) as for the reference of the free dye (74.5±15.1). These both values are statistically identical (p>0.05). One possible explanation could be that a long cycle affected the photo-chemical features of the fluorescein dye when attached to aptamer and consequently induced both a decrease in the fluorescence anisotropy and a higher variability in all signals (Perrier *et al.*, 2009). Dye played a preponderant role in the performance of the FP assays (Perrier *et al.*, 2018).

K_d values of flight ñupper & lower trayò samples are not statistically different from ground ñDLR 5°Cò and ñCNES 5°Cò controls. Consequently, based on the above considerations, our

403 results showed that aptamer recognition capabilities were not affected during the overall flight
404 mission or that the degradations are too small to be detected by our analysis protocol.

IV. Conclusions

During the last years, we used various facilities producing protons, electrons, neutrons and heavy ions to test whether cosmic particles could induce changes in aptamer binding events. However, simulating space radiation environment in Earth facilities remains impossible due to the great number of variables. So, we also carried out a real space exposure of aptamer samples outside the ISS during the EXPOSE-R2 mission.

The results presented in this paper suggest that cosmic radiation has no significant effect on the aptamers recognition ability. On the contrary, repeated temperature cycling seems to alter the mobility of its fluorescein dye. This effect results in a lowering of the recognition step signal that could be interpreted as a loss of recognition, or as the absence of the target, or as an alteration of the fluorescent dye properties. In all cases, it alters the limit of detection of the biochip.

In our context, since we controlled the concentration of the target and we obtained K_d values similar to the reference value, we attribute the lowering of signal as a modification of fluorescent dye mobility. So, we suggest conducting further studies to improve the detection step using another fluorescent dye or another detection method.

Acknowledgments

The authors would like to thank the French national space agency (CNES) for financial support (05/2182/00-DCT094). The authors also thank all staff from the Louvain-la-Neuve cyclotron facility, from the Bergonié Institut, and the staff from the Istituto Nazionale di Fisica Nucleare of Catania for their assistance during irradiation experiments. The authors thank Jean-Louis Kergueme from the Mechanics Department of the Montpellier University for his assistance

during the desoldering of the CNES cells, and Dr. Sonia Khier for her assistance that has led to good progress during the analysis of samples.

References

Baqué, M., Le Postollec, A., Coussot, G., Moreau, T., Desvignes, I., Incerti, S., Moretto, P., Dobrijevic, M., Vandenabeele-Trambouze, O. (2011a) Biochip for astrobiological applications: Investigation of low energy protons effects on antibody performances. *Planetary and Space Science* 59(13):1490 ï 1497.

Baqué, M., Le Postollec, A., Ravelet, C., Peyrin, E., Coussot, G., Desvignes, I., Incerti, S., Moretto, P., Dobrijevic, M., Vandenabeele-Trambouze, O. (2011b) Investigation of Low-Energy Proton Effects on Aptamer Performance for Astrobiological Applications. *Astrobiology* 11(3): 207ï 211.

Baqué, M., Dobrijevic, M., Le Postollec, A., Moreau, T., Faye, C., Vigier, F., Incerti, S., Coussot, G., Caron, J., Vandenabeele-Trambouze, O. (2017) Irradiation effects on antibody performance in the frame of biochip-based instruments development for space exploration. *International Journal of Astrobiology* 16(1): 82-90.

Berger, T., Hajek, M., Bilski, P., Koerner, C., Vanhavere, F., Reitz, G. (2012). Cosmic radiation exposure of biological test systems during the EXPOSE-E mission. *Astrobiology* 12(5): 387ï 392.

Berger, T., Hajek, M., Bilski, P., Reitz, G. (2015). *Cosmic radiation exposure of biological test systems during the EXPOSE-R mission. International Journal of Astrobiology*, 14(1), 27-32

Cottin, H., Saiagh, K., Nguyen, D., Grand, N., Benilan, Y., Cloix, M., Coll, P., Gazeau, M-C., Fray, N., Khalaf, D., Raulin, F., Stalport, F., Carrasco, N., Szopa, C., Chaput, D., Bertrand, M., Westall, F., Mattioda, A., Quinn, R., Ricco, A., Santos, O., Baratta, G., Strazzulla, G., Palumbo, M.E., Le Postollec, A., Dobrijevic, M., Coussot, G., Vigier, F., Vandenabeele-Trambouze, O., Incerti, S., Berger, T. (2015) Photochemical studies in low Earth orbit for organic compounds related to small bodies, Titan and Mars. *Current and future facilities*, Bulletin de la Société Royale des Sciences de Liège 84 : 60-73.

Cottin, H., Kotler, J.M., Billi, D., Cockell, C., Demets, R., Ehrenfreund, P., Elsaesser, A., dôHendecourt, L., van Loon, J.J.W.A., Martins, Z., Onofri, S., Quinn, R.C., Rabbow, E., Rettberg, P., Ricco, A.J., Slenzka, K., de la Torre, R., de Vera, J.-P., Westall, F., Carrasco, N., Fresneau, A., Kawaguchi, Y., Kebukawa, Y., Nguyen, D., Poch, O., Saiagh, K., Stalport, F., Yamagishi, A., Yano, H. and Klamm, B.A. (2017) Space as a Tool for Astrobiology: Review and Recommendations for Experimentations in Earth Orbit and Beyond. Space Science Reviews 209, 83-181.

Coussot, G., Moreau, T., Faye, C., Vigier, F., Baqué, M., Le Postollec, A., Incerti, S., Dobrijevic, M., Vandenabeele-Trambouze, O. (2017) Biochip-based instruments development

for space exploration: influence of the antibody immobilization process on the biochip resistance to freeze-drying, temperature shifts and cosmic radiations. *International Journal of Astrobiology* 16(2):190-199.

Coussot, G., Faye, C., Le Postollec, A., Dobrijevic, M. (2018a) A methodological approach for the thermal stability and stress exposure studies of a model antibody. *Analytical Biochemistry*, 548: 23-31.

Coussot G., Le Postollec A., Faye C., Baqué M., Vandenabeele-Trambouze O., Incerti S., Vigier F., Chaput D., Cottin H., Przybyla B., Berger T., Dobrijevic M. (2018b) Photochemistry on the Space Station - Antibody resistance to space conditions after exposure outside the International Space Station. *Astrobiology*, in press.

de Diego-Castilla, G., Cruz-Gil, P., Mateo-Martí, E., Fernández-Calvo, P., Rivas, L.A., Parro, V. (2011) Assessing antibody microarrays for space missions: effect of long-term storage, gamma radiation, and temperature shifts on printed and fluorescently labeled antibodies. *Astrobiology* 11(8):759ï 773.

Derveni, M., Allen, M., Sawakuchi, G.O., Yukihara, E.G., Richter, L., Sims, M.R., Cullen, D.C. (2013) Survivability of immunoassay reagents exposed to the space radiation environment on board the ESA BIOPAN-6 Platform as a prelude to performing immunoassays on Mars. *Astrobiology* 13(1):93-102.

Derveni, M., Hands, A., Allen, M., Sims, M.R., & Cullen, D.C. (2012) Effects of simulated space radiation on immunoassay components for Life-detection experiments in planetary exploration missions. *Astrobiology* 12(8): 718ï 729.

Dong, Y., Xu, Y., Yong, W., Chu, X., Wang, D. (2014) Aptamer and its potential applications for food safety. *Critical Reviews in Food Science and Nutrition*. 54(12): 1548-1561.

Gotrik, M.R., Feagin, T.A., Csordas, A.T., Nakamoto, M.A., Soh, H.T (2016) Analysis of aptamer discovery and technology. *Accounts of chemical research* 49(9):1903-1910.

Hassler, D M., Zeitlin, C., Wimmer-Schweingruber, R F.; Ehresmann, B.; Rafkin, S.; Eigenbrode, J L.; Brinza, D E.; Weigle, G.; Böttcher, S.; Böhm, E.; and 438 coauthors (2014) Mars' Surface Radiation Environment Measured with the Mars Science Laboratory's Curiosity Rover. *Science* 343 (6169), id. 1244797.

Le Postollec, A. , Dobrijevic, M., Incerti, S., Moretto, P., Seznec, H., Desorgher, L., Santin, G., Nieminen, P., Dartnell, L., Vandenabeele-Trambouze, O., Coussot, G. (2007) Development of a Biochip dedicated to planetary exploration. First step: resistance studies to space conditions. Journées Semaine de lôAstrophysique Française 2007.

Le Postollec, A., Incerti, S., Dobrijevic, M., Desorgher, L., Santin, G., Moretto, P., Vandenabeele-Trambouze, O., Coussot, G., Dartnell, L., Nieminen, P. (2009a) Monte Carlo simulation of the radiation environment encountered by a biochip during a space mission to Mars. *Astrobiology* 9(3): 311ï 323.

Le Postollec, A., Coussot, G., Baqué, M., Incerti, S., Desvignes, I., Moretto, P., Dobrijevic, M., Vandenabeele-Trambouze, O. (2009b) Investigation of Neutron Radiation Effects on Polyclonal Antibodies (IgG) and Fluorescein Dye for Astrobiological Applications. *Astrobiology* 9(7): 637ï 645.

Martins, Z. (2011) In situ biomarkers and the Life Marker Chip. *Astronomy & Geophysics* 52(1):1.34 - 1.35.

McKay, C.P.,Stoker, C.R., Glass, B.J., Davé, A., Davila, A.F., Heldmann, J.L., Marinova, M.M., Fairen, A.G., Quinn, R.C., Zacny, K.A., Paulsen, G., Smith, P.H., Parro, V., Andersen, D.T., Hecht, M.H., Lacelle, D., Pollard, W.H. (2013) The Icebreaker Life Mission to Mars: A Search for Biomolecular Evidence for Life. *Astrobiology* 13(4): 334ï 353.

McKenna-Lawlor, S., Gonçalves, P., Keating, A., Reitz, G., Matthiä, D. (2012) Overview of energetic particle hazards during prospective manned missions to Mars. *Planetary and Space Science* 63ï 64(0): 123ï 132.

Parro, V., Rodriguez-Manfredi, J.A., Briones, C., Compostizo, C., Herrero, P.L., Vezb, E., Sebastián, E., Moreno-Paz, M., García-Villadangos, M., Fernández-Calvo, P., González-Toril, E., Pérez-Mercader, J., Fernández-Remolar, D., Gómez-Elvira, J. (2005) Instrument development to search for biomarkers on mars: Terrestrial acidophile, iron-powered chemolithoautotrophic communities as model systems. *Planetary and Space Science* 53(7):729-737.

Parro, V., Fernández-Remolar, D., Rodríguez-Manfredi, J.A., Cruz-Gil, P., Gómez-Elvira, J. (2008) SOLID2: an antibody array-based Life-detector instrument in a Mars drilling simulation experiment (MARTE). *Astrobiology* 8(5): 987ï 999.

Parro, V., Fernández-Remolar, D., Rodríguez-Manfredi, J.A., Cruz-Gil, P., Rivas, L.A., Ruiz-Bermejo, M., Moreno-Paz, M., García-Villadangos, M., Gómez-Ortiz, D., Blanco-López, Y., Menor-Salván, C., Prieto-Ballesteros, O., Gómez-Elvira, J. (2011a) Classification of modern and Old Rio Tinto sedimentary deposits through the biomolecular record using a Life Marker Biochip: Implications for detecting life on Mars. *Astrobiology* 11(1): 29ï 44.

Parro, V., de Diego-Castilla, G., Rodríguez-Manfredi, J.A. , Rivas, L.A., Blanco-López, Y., Sebastián, E., Romeral, J., Compostizo, C., Herrero, P.L., García-Marín, A., Moreno-Paz, M., García-Villadangos, M., Cruz-Gil, P., Peinado, V., Martín-Soler, J., Pérez-Mercader, J.,

Gómez-Elvira, J. (2011b) SOLID3: a multiplex antibody microarray-based optical sensor instrument for in situ Life detection in planetary exploration. *Astrobiology* 11(1): 15ï 28.

Perrier, S., Ravelet, C., Guieu, V., Roy, B., Perigaud, C., Peyrin, E. (2010) Rationally designed aptamer-based fluorescence polarization sensor dedicated to the small target analysis. *Biosensors & Bioelectronics* 25:1652ï 1657.

Perrier, S., Guieu, V., Chovelon, B., Ravelet, C., Peyrin, E. (2018) Panoply of fluorescence polarization/anisotropy signaling mechanisms for functional nucleic acid-based sensing platforms. *Analytical Chemistry* 90: 4236-4248.

Rabbow, E., Rettberg, P., Parpart, A., Panitz, C., Schulte, W., Molter, F.,Willnecker, R. (2017). EXPOSE-R2: The Astrobiological ESA Mission on Board of the International Space Station. *Frontiers in Microbiology*, 8, 1533. http://doi.org/10.3389/fmicb.2017.01533.

Rozenblum, G.T., Lopez, V.G., Vitullo, A.D., Radrizzani, M. (2016) Aptamers: current challenges and future prospects. *Expert Opinion on Drug Discovery* 11(2): 127-135.

Ruta, J., Perrier, S., Ravelet, C., Fize, J., Peyrin, E. (2009) Noncompetitive fluorescence polarization aptamer-based assay for small molecule detection. *Analytical Chemistry* 81:7468ï 7473.

Sims, M.R., Pullan, D., Holt, J., Blake, O., Sykes, J., Samara-Ratna, P., Canali, M., Cullen, D.C., Rix, C.S., Buckley, A., Derveni, M., Evans, D., Miguel García-Con, L., Rhodes, A., Rato, C.C., Stefinovic, M., Sephton, M.A., Court, R.W., Bulloch, C., Kitchingman, I., Ali, Z., Borst, G., Leeuwis, H., Prak, A., Norfini, A., Geraci, E., Tavanti, M., Brucato, J., Holm, N. (2012) Development status of the life marker chip instrument for ExoMars. *Planetary and Space Science* 72(1): 129ï 137.

Smith, H., Parro, V. (2014) Planetary Protection Plan for an Antibody based instrument proposed for Mars2020. *in 40th COSPAR Scientific Assembly*. p. 3140.

Song, K-M., Lee, S., Ban, C. (2012) Aptamers and Their Biological Applications, *Sensors (Basel)* 12(1): 612ï 631.

Vigier, F., Le Postollec, A., Coussot, G., Chaput, D., Cottin, H., Berger, T., Triqueneaux, S., Dobrijevic, M., Vandenabeele-Trambouze, O. (2013) Preparation of the Biochip experiment on the EXPOSE-R2 mission outside the International Space Station. *Advances in Space Research* 52(12): 2168ï 2179.

Zhu, Z., Schmidt, T., Mahrous, M., Guieu, V., Perrier, S., Ravelet, C., Peyrin, E. (2011) Optimization of the structure-switching aptamer-based fluorescence polarization assay for the sensitive tyrosinamide sensing. *Analytica Chimica Acta* 707: 191-196.

Figures

Figure 1

1a)

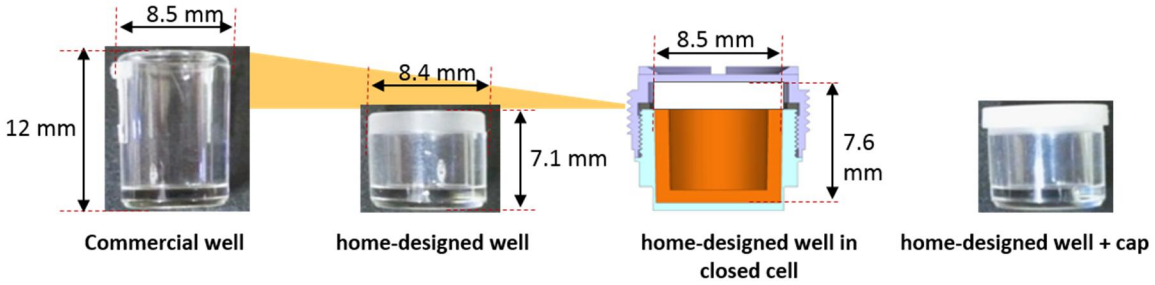

1b)

1c)

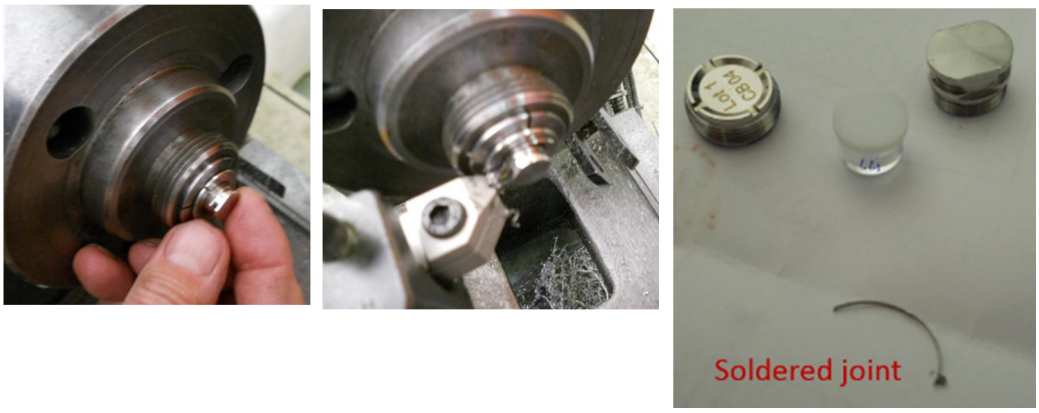

Figure 1 caption:

1a) Design and dimension of the home-designed well and its cap.

1b) Incorporation of capped well into CNES cells under controlled atmosphere and final screwing of closed CNES cells using a torque screwdriver.

1c) Post-flight opening of the CNES cells to remove the soldered joint.

Figure 2

2a)

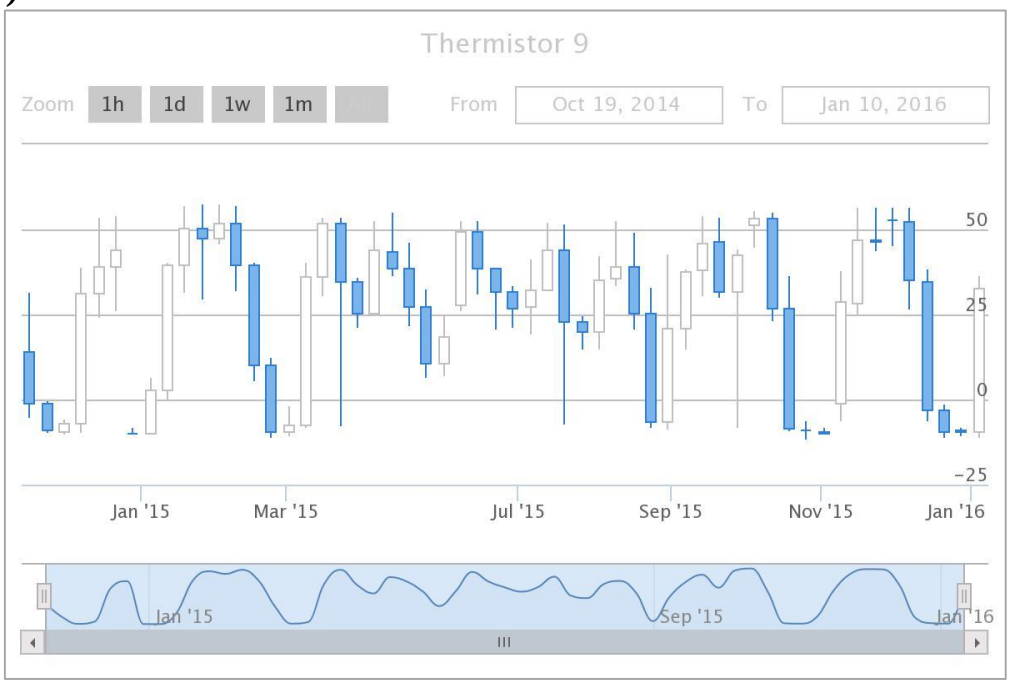

2b)

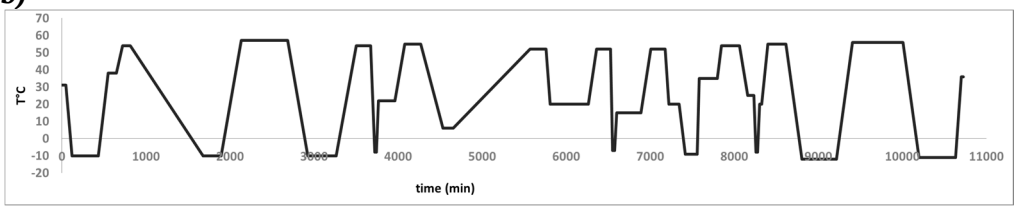

Figure 2 caption:

2a) Overview of the EXPOSE-R2 temperature profiles for tray 3 on thermistor 9 sensor during the EXPOSE-R2 mission (from October 19, 2014 to January 10, 2016, http://www.musc.dlr.de/expose-r-2/).

2b) Ground thermal cycling experiments mimicking thermal CNES cells exposure outside the ISS but in accelerated time: one hour of EXPOSE-R2 mission was converted into one minute to carry out this experiment in lab, and temperature amplitude was similar (referred as long cycle in the text).

Figure 3

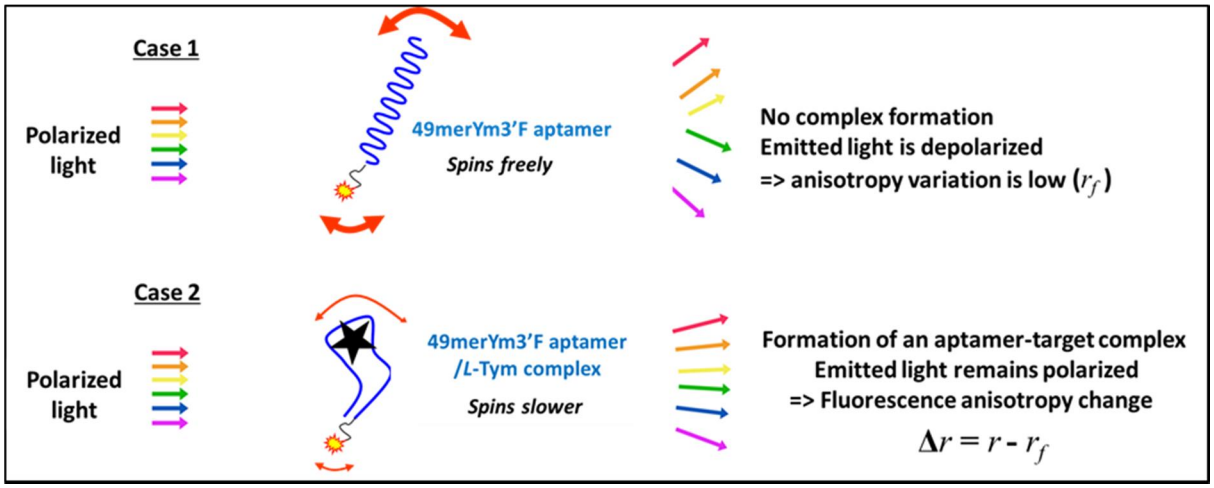

Figure 3 caption: Principle of the fluorescence polarization (FP) assays. A fluorescence anisotropy increase is observed upon the formation of a labelled aptamer-target complex.

Figure 4

4a)

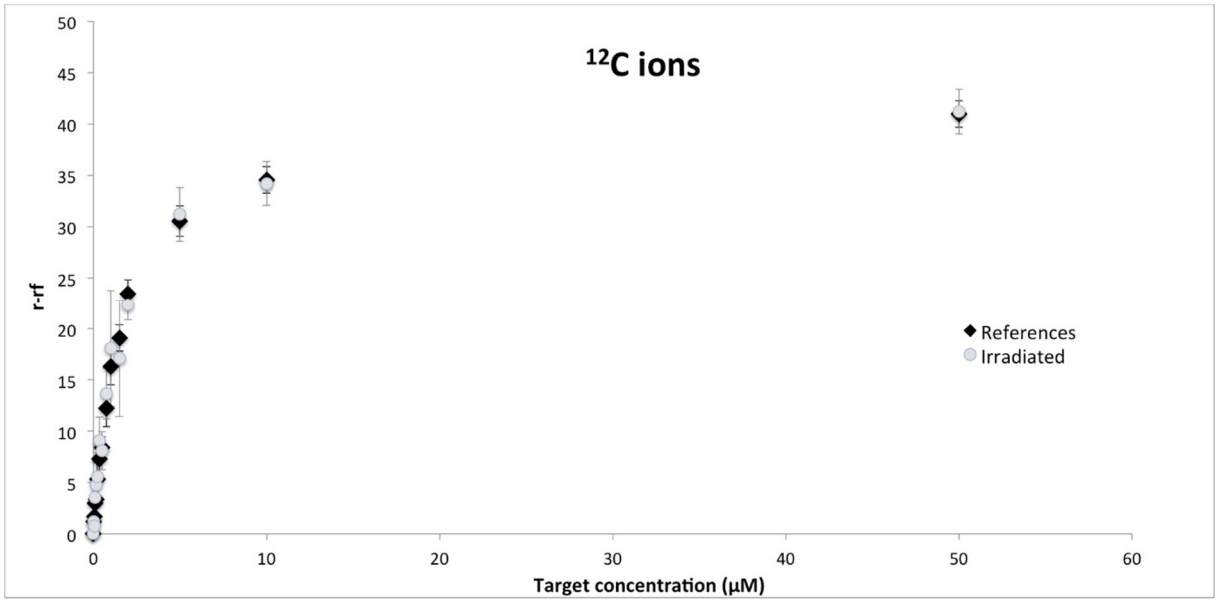

4b)

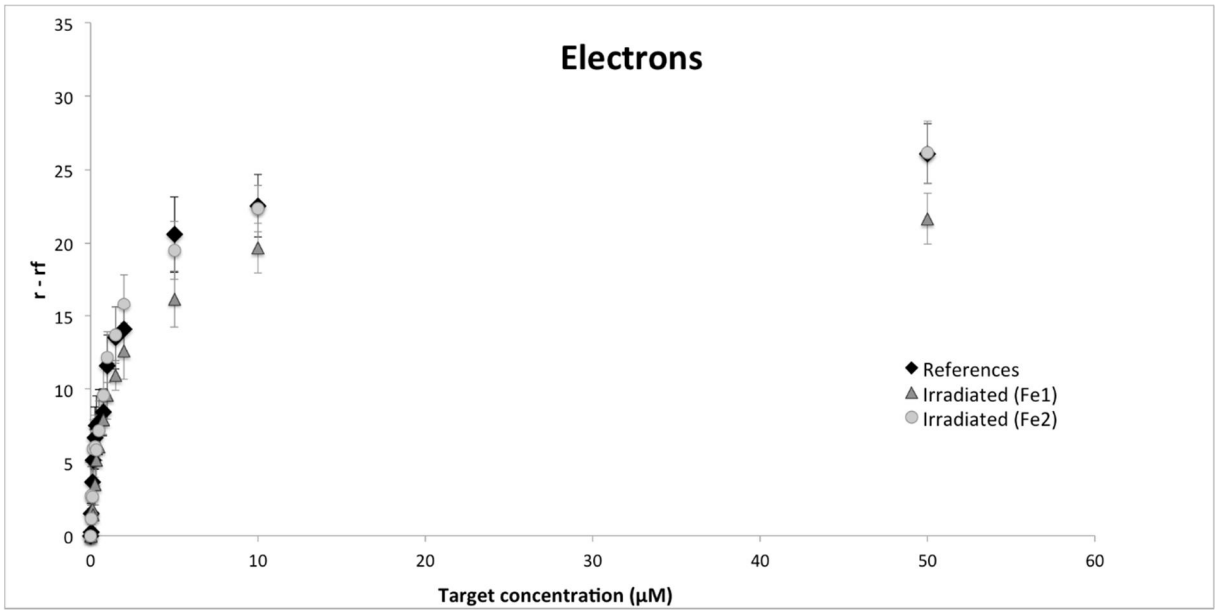

682 ***4c)***

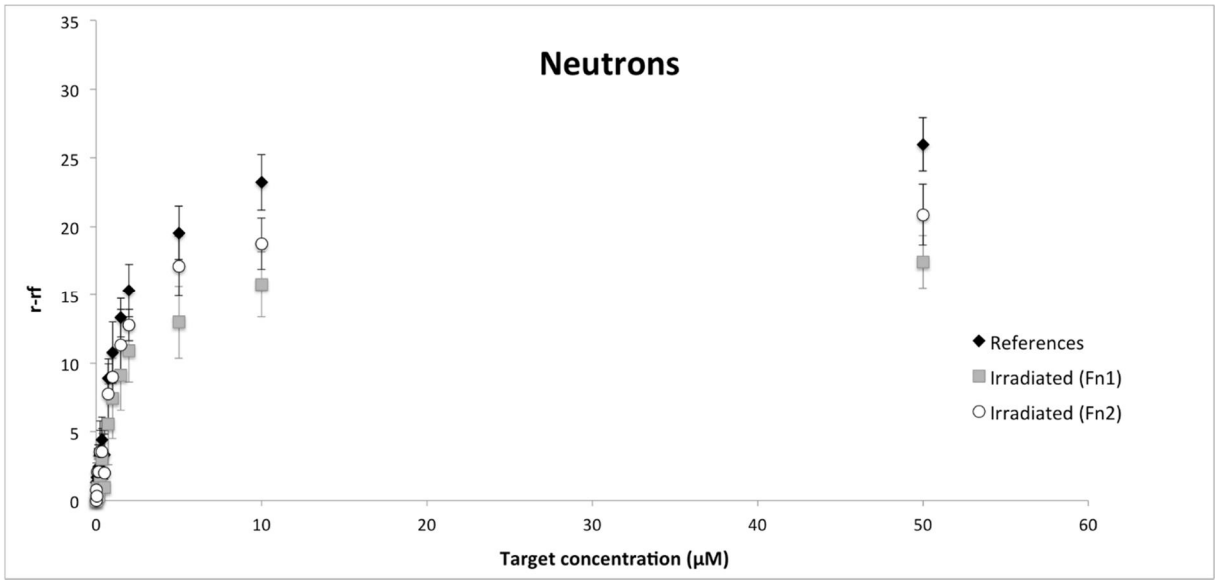

683

684

685 ***4d)***

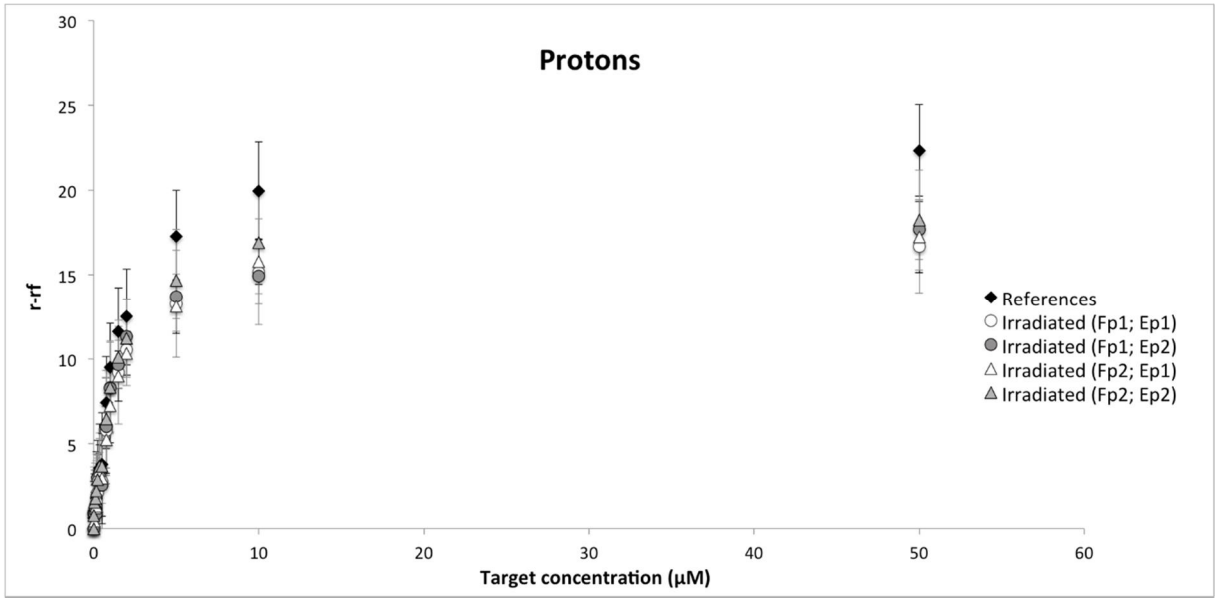

686

687 **Figure 4 caption:** Affinity curves for 49merYm3ôF aptamer with additions of *L*-Tym
688 obtained for reference (non irradiated sample), and irradiated samples with particles at various
689 fluence (F), energy (E), and irradiation duration (D), (for details see Table 1). The saturation
690 curves were used for the determination of dissociation constant values (Kd) (Eq. 2) by non-
691 linear regression analysis. The calculated relative Kd are listed in Table 2. Reference samples
692 (n=3 or 6) are labelled in black diamond.

4a) Irradiated samples with 12C ions (Fc;Ec; Dc) are illustrated in grey cycle (n=3). 4b) Irradiated samples are represented in dark grey triangle with electron fluences of 3.1011 p/cm2 (Fe1; n=4) and with a grey circle for 3.1010 p/cm2 fluence (Fe2; n=4).

4c) Irradiated samples with neutron fluences of 3.1013 p/cm2 (Fn1; n=3) are illustrated in grey square, and 3.1012 p/cm2 (Fn2; n=3) in empty circle.

4d) Irradiated sample with protons fluence of 3.1012 p/cm2 with energy of 25 MeV (Fp1; Ep1; n=3) are represented in empty circle, and in grey circles for an energy of 50 MeV (Fp1; Ep2; n=3). Fluence of 3.1011 p/cm2 with energy of 25 MeV (Fp2; Ep1; n=3) are plotted with an empty triangle, and with an energy of 50 MeV (Fp2; Ep2; n=3) with a grey triangle.

Figure 5

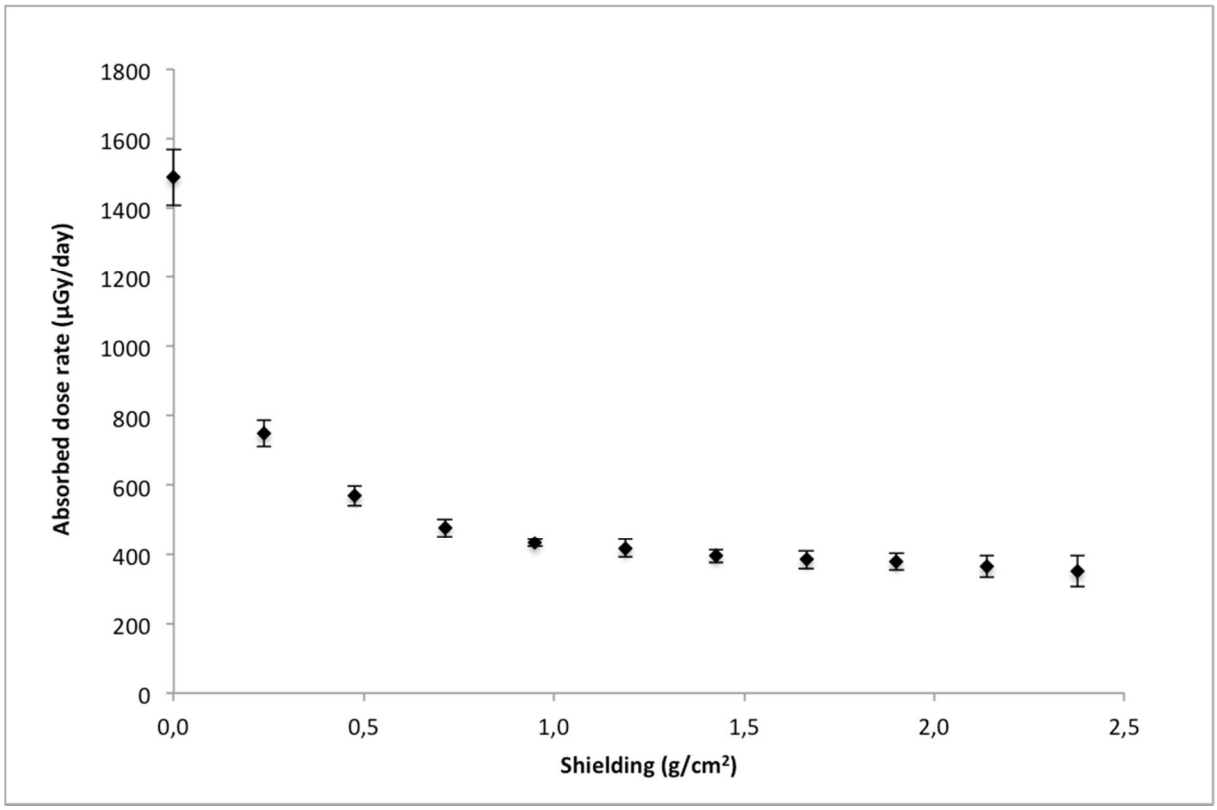

Figure 5 caption: Evolution of the absorbed dose rate as a function of the shielding. Measurements were performed on 5 stacks of 11 TLDs placed into the Tray 3 during EXPOSE-R2 mission.

712 **Figure 6**

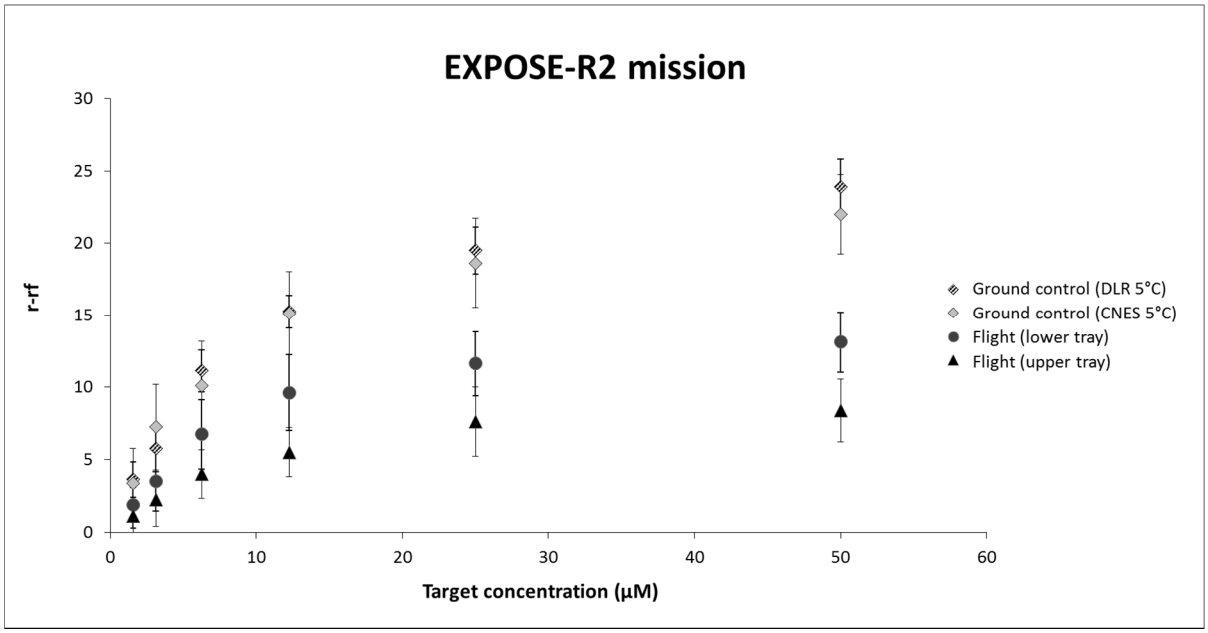

713
714

715 **Figure 6 caption:** Affinity curves for 49merYm3ôF aptamer with additions of L-Tym
716 obtained for controls and flight samples. The corresponding relative Kd values are given in
717 Table 3.
718

Table 1

Date	Place		Particule type	Fluence (particules/cm^2)	Energy	Irradiation duration
04/27/2012	Istituto Nazionale di Fisica Nucleare	Catania, Italy	^{12}C	$F_c = 2.10^6$	E_c = 62 MeV/nuc	D_c = 7 min
07/07/2011	Institut Bergonié	Bordeaux, France	Electrons	$F_{e1} = 3.10^{11}$ $F_{e2} = 3.10^{10}$	E_e = 9 MeV	D_{e1} =70 min D_{e2} =7 min
06/01/2010	Centre de Recherche du Cyclotron	Louvain-la-Neuve, Belgium	Neutrons	$F_{n1} = 3.10^{13}$ $F_{n2} = 3.10^{12}$	E_n = 17 MeV (mean)	D_n = 22 min
03/06/2010			Protons	$F_{p1} = 3.10^{12}$ $F_{p2} = 3.10^{11}$	E_{p1} = 25 MeV E_{p2} = 50 MeV	D_{p1} = 1h40min D_{p2} = 10 min

Table 1 caption Main experimental conditions for neutron, proton, electron and carbon ions irradiations. Subscript letters indicate the particle type and subscript numbers are used to differentiate the applied conditions. Units for fluences are in particles per cm^2. Technical details have already been reported in Baqué *et al.* studies (Baqué *et al.*, 2017).

Table 2

Experiments on ground-based particles accelerator facilities	
Particle type	relative K_d for irradiated samples (fluence, energy, duration, replicates)
^{12}C	1.01± 0.15 (F_c; E_c; D_c; 3)
Electrons	1.09± 0.22 (F_{e1}; E_e; D_{e1}; 4) 0.99± 0.20 (F_{e2}; E_e; D_{e2}; 4)
Neutrons	1.19± 0.35 (F_{n1}; E_n; D_n; 3) 0.99± 0.16 (F_{n2}; E_n; D_n; 3)
Protons	0.88± 0.21 (F_{p1}; E_{p1}; D_{p1}; 3) 0.80± 0.15 (F_{p1}; E_{p2}; D_{p1}; 3) 0.93± 0.18 (F_{p2}; E_{p1}; D_{p2}; 3) 0.84± 0.16 (F_{p2}; E_{p2}; D_{p2}; 3)

Table 2 caption: Relative dissociation constant values (relative K_d) (Eq. 2) derived from the titration curves obtained for irradiated samples (n=3 or 4) after ground-based irradiation experiments with at least (n=3) reference samples.

Table 3

Biochip in PSS experiment during the EXPOSE-R2 mission	
Sample type	relative K_d (replicates)
Ground control (CNES 5°C)	0.82± 0.10 (2)
Ground control (DLR 5°C)	1.00± 0.10 (2)
Ground control (DLR ΔT)	1.29± 0.28 (1)
Ground control (DLR ΔT + UV)	0.93± 0.20 (2)
Flight (upper tray)	0.94± 0.14 (2)
Flight (lower tray)	1.07± 0.21 (2)

Table 3 caption: Relative dissociation constant values (relative K_d) (Eq. 2) derived from the titration curves issued from the ñBiochip in PSS experimentò during the EXPOSE-R2 mission.